APPLICATION OF MICRO-RAMAN SPECTROSCOPY FOR THE IDENTIFICATION OF UNCLASSIFIED MINERALS PRESERVED IN OLD MUSEUM COLLECTIONS

PAOLO MAZZOLENI[1], GERMANA BARONE[1], SIMONA RANERI[1], ERICA AQUILIA[1], DANILO BERSANI[2], ROSOLINO CIRRINCIONE[1]

[1] Dipartimento di Scienze Biologiche, Geologiche e Ambientali (BiGeA), Università di Catania, Corso Italia 57, 95129 Catania

[2] Dipartimento di Fisica e Scienze della Terra, Università di Parma, Parco Area delle Scienze 7/A, 43124 Parma

ABSTRACT

Minerals collections represent a relevant cultural resource in the framework of the diffusion of scientific and technological knowledge. In this perspective, the correct classification and cataloguing of mineralogical materials is mandatory in the staging of temporary exhibitions and Natural History Museums. As the relevance of the collections, often represented by rare and really valuable samples coming from worldwide geological sites, the characterization and identification of mineralogical species requires the use of non-invasive and non-destructive techniques; among them, Raman-spectroscopy represents a really useful tool in mineralogical studies.

The Department of Biological, Geological and Environmental Sciences (DBiGeA) of the University of Catania preserves several mineralogical collections acquired over the time by private and researcher donations. In view of the new staging of the Mineralogical Museum and the requirement of a correct cataloguing and characterization of several unclassified minerals, a library of Raman spectra compiled by using 785 nm excitation line has been realized with the aim to support the exhibition of the materials. In particular, an interesting set of phosphates, arsenates, and vanadates class minerals (08; Nickel-Strunz Classification), relevant in the framework of collecting and ore research, have been analysed; among them, mineralogical samples of rashleighite-turquoise and purpurite, whose Raman spectra are not available in the databases, have been identified, allowing the enlargement of RRUFF online project.

The overall of the obtained results allow us to classify numerous samples and re-classify mistaken attribution, highlighting also the potential of Raman spectroscopy in fast and *on-site* identification of mineralogical materials.

INTRODUCTION

According to the Cataloguing and Documenting Institute of the Italian Ministry of Cultural Heritages, mineral collections constitute Naturalistic Heritages (AA.VV., 2009) that have to be maintained and used for didactic, research and cultural purposes in view of the diffusion of the scientific knowledge. In this framework, the correct nomenclature and cataloguing of minerals represents a mandatory requirement for their valorization and fruition. Really interesting mineral collections are preserved in several Earth Science Research Institutions and exhibited in Natural Museums (Kohlstedt, 1988). In view of the presence of rare minerals of a great scientific interest, these collections represent a really valuable heritage for students, researchers, users and collectors. However, in many cases, they include old specimens classified following outdated schemes; furthermore, the frequent reshuffle of the exhibitions and the documental archives often causes a loss of classification and provenance information of minerals.

The DBiGeA of the Catania University owns rich collections consisting in thousands of minerals; the oldest one is represented by minerals and rocks offered to the University by Giuseppe Gioieni and Principe di Biscari in 1781. During the new staging of the Mineralogical Museum of the Department, about a thousand of minerals have been found in the archives; among them, a large number of mineral samples unclassified and/or

equipped with unclear archive tags have been discovered. In view of their exhibition, a correct classification and nomenclature was required; moreover, being part of collections, the use non-destructive, fast and cheap analyses was mandatory.

In this context, Raman spectroscopy represents a really useful tool, as testified by numerous application of the method in mineralogical studies (Nasdala *et al.*, 2004) as well as the development of several projects finalized to create online databases for the open access of data. Moreover, the potential of Raman spectroscopy for geological aims has been greatly highlighted by the recent scientific literature; for instance, Jehlička *et al.* (2009) used portable Raman spectrometers for the non-destructive detection of minerals on outcrops whereas Hope *et al.* (2001) and Vítek *et al.* (2012) investigated the potential of portable Raman spectroscopy for the identification of minerals from mineralogical collections. Finally, several authors focused their researches in inspecting the potential of Raman spectroscopy for the characterization of minerals having archaeological (Adriaens, 2005; Bouchard & Smith, 2003; Burgio & Clark, 2001; Smith & Clark, 2004; Vandenabeele, 2004), gemological (Barone *et al.*, 2014, 2015; Bersani *et al.*, 2014) and environmental significance (Frost *et al.*, 2003).

In this work, micro-Raman measurements have been carried out on a selection of mineralogical samples discovered in the archives of the DBiGeA Mineralogical Museum; the obtained results have allowed us to identify numerous minerals, reclassify mistaken attributions and confirm previous identifications. On the basis of the analyses performed on minerals, a new classification has been therefore obtained, making the materials available for scientific, expositive and didactic purposes and supporting the exhibitions at the DBiGeA Mineralogical Museum.

MATERIALS AND METHODS

Among the thousands of minerals discovered in the archives, 46 unclassified and misclassified mineralogical materials have been selected for micro-Raman analysis, in view of their exhibition at the Museum. The majority of them were lacking of appropriate tag and/or catalogue numbering, avoiding any identification of both mineralogical species and provenance. It is noteworthy that the systematic cataloguing of the collections of the Department has started in 1912; therefore, samples devoid of track number could be related to previous donation and/or acquisition. Only in rare cases, information on mineral species were provided; however, as the inconsistencies between macroscopic features of minerals and the reported information, these samples have been analysed in order to verify the reliability of the archive data.

In Annex 1 a list of analysed minerals is reported, with a detailed description of some proprieties determined by preliminary macroscopic analysis as luster, color, diaphaneity and fracture.

On the selected samples, micro-Raman spectra have been collected by means of a micro-Raman Jasco NRS-3100 apparatus equipped with a microscope with 10x, 20x and 100x objectives and two laser excitation sources at 532 and 785 nm; the excitation line at 785 nm has been used for these measurements. Laser power has been controlled by means of a series of density filters (ND), to avoid heating effects. The maximum laser power at the sample was less than 10 mW. The minimum lateral and depth resolutions were set both to about 1 μm by means of a confocal hole. The systems have been calibrated using the 520.7 cm^{-1} Raman band of silicon before each experimental session. All the experimental Raman spectra have compared with data from various databases and literature (RRUFF; Handbook of Minerals Raman spectra, Lyon; Minerals Raman Database, University of Parma) in order to identify the composition of studied minerals.

Finally, only in rare cases, for which reference Raman spectra were not available in the online databases, X-ray diffraction (XRD) analyses have been performed. In detail, XRD data have been collected by using a SIEMENS D 5000 with Cu-Kα radiation and an Ni filter. Randomly oriented powders have been scanned from 2° to 45° 2θ, with a 0.02° 2θ step size with a counting time of 2 s per step. The tube current and the voltage were 30 mA and 40 kV, respectively.

RESULTS AND DISCUSSION

Unclassified minerals

Twenty-four mineralogical samples selected for the analyses were lacking of archive tags; for these materials, therefore, no information about composition, geographical provenance and collection identity were available. The analyses performed by micro-Raman have allowed us to identify several classes of minerals, namely oxides (04; Nickel-Strunz Class.), carbonates (05; Nickel-Strunz Class.), silicates (09; Nickel-Strunz Class.), sulfides (02; Nickel-Strunz Class.), phosphates (08; Nickel-Strunz Class.) and halides (03; Nickel-Strunz Class.), as well as native elements. Raman features obtained from the analysis of the acquired spectra are reported in Annex 2, with the relative attribution and the new cataloguing information achieved thanks to the identification of the studied mineralogical samples.

Among the oxides, beside several examples of macrocrystalline and prismatic white crystals of quartz, numerous hematite samples exhibiting a wide range of colors and crystal habits have been identified, as in the case of the sample labeled as M13, for which the presence of Raman peaks at 295, 408, 552 and 614 cm^{-1} allow to classify it as iridescent hematite associated with goethite.

The category of carbonate minerals comprises examples of different calcium carbonate polymorphs, well distinguishable by using Raman spectroscopy, as well as rare and valuable minerals. Among the latter ones, noteworthy is a sample of sphaerocobaltite (labeled as M5), a rare cobalt carbonate mineral in which the presence of impurities determines a wide variety of red shades (Fig. 1a).

The mineralogical class of silicate is represented by a mica (M4) and a zeolite (M7) samples; for the former, the Raman spectrum collected on mineral highlights the typical modes at 410, 560 and 710 cm^{-1} of lepidolite (Fig. 1b), a violet to pink variety of mica widely used for gemological purposes.

Referring to sulphate class, a really valuable and exquisite example of celestine (Fig. 1c) has been recognized among the unclassified minerals (sample M12), as testified by its Raman spectrum that exhibits bands at 453, 624 and 1000 cm^{-1} attributed to SO_4 symmetric banding (sym. band.), anti-symmetric banding (anti. band.) and symmetric stretching (sym. stretch.) modes, respectively (Periasamy *et al.*, 2009).

Finally, really interesting minerals belonging to phosphates and arsenates mineralogical class have been identified; noteworthy is a very interesting sample of carminite (labelled as M23; Fig. 1d), a rare secondary mineral formed as an alteration product of arsenopyrite in the oxidized zones of lead-bearing deposits, whose Raman spectrum exhibits the typical AsO_4 vibrational frequencies at 211, 260, 350, 380, 464, 497, 547, 740, 810, 850 cm^{-1} (Frost & Kloprogge, 2003).

Reclassification of mistaken attribution and confirmation of previous identification

For twenty-two specimens an archive tag supplying data about mineralogical species without any indications on provenance and collection has been found; however, in some cases, the inconsistency between physical features detected by macroscopic analysis and information reported on the badges has suggested a mistaken attribution of samples. In this framework, micro-Raman analyses have allowed the reclassification of eight minerals (M25-M33), while for the other ones (M34-M46) the collected spectroscopic data have confirmed the archive identification (see Annex 2).

Reclassified samples consist mainly in carbonates (05; Nickel-Strunz Class.), oxides (04; Nickel-Strunz Class.) and halides (03; Nickel-Strunz Class). For these materials, the incorrect classification can be attributed to a mix up of the badges during the numerous reshuffle of the collections, over the time. Among them, have to be mentioned an interesting sample of black quartz (M26), previously classified as pyromorphite (Fig. 2a), and a really exquisite geode (sample M28; archive tag: fluorite) characterized by white/pale-rose shell lines and crystals identified as dolomite. In other cases, features as color and luster probably misled the ancient curators of the Mineralogical Museum, even if a mix up of badges cannot be excluded, too; an example is represented by the sample labeled as M27 and previously classified as barthite, whose Raman spectrum exhibits features at 152, 176, 218, 266, 346, 429, 531, 717, 1059 and 1092 cm^{-1}, typical of malachite (Fig. 2b).

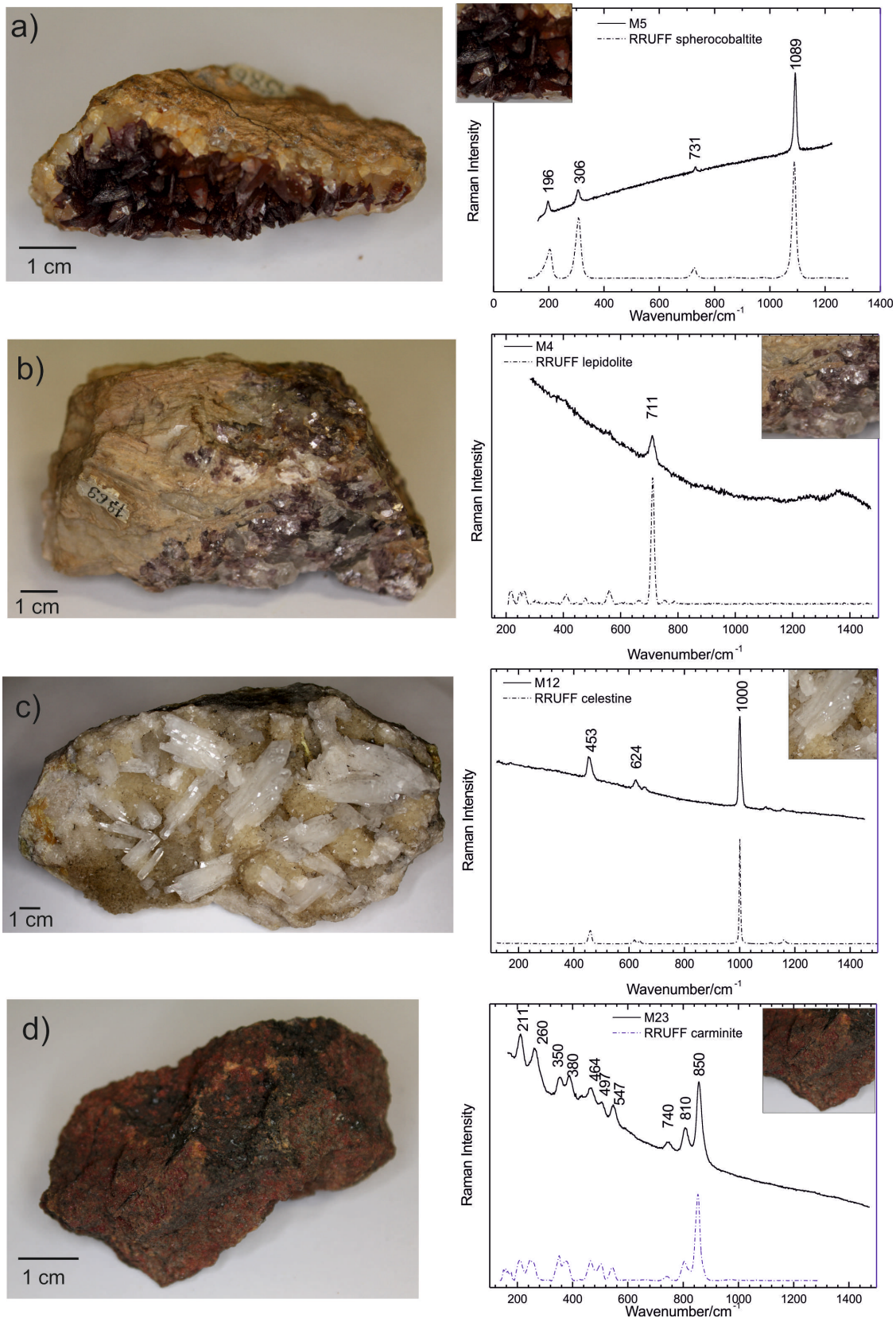

Fig. 1 - Picture and micro-Raman spectra acquired by using 785 nm excitation line on some unclassified materials, as examples. (a) carbonate: sample M16, spherocobaltite; (b) silicate: sample M4, lepidolite; (c) sulphate: sample M12, celestine; (d) phosphate: sample M23, carminite.

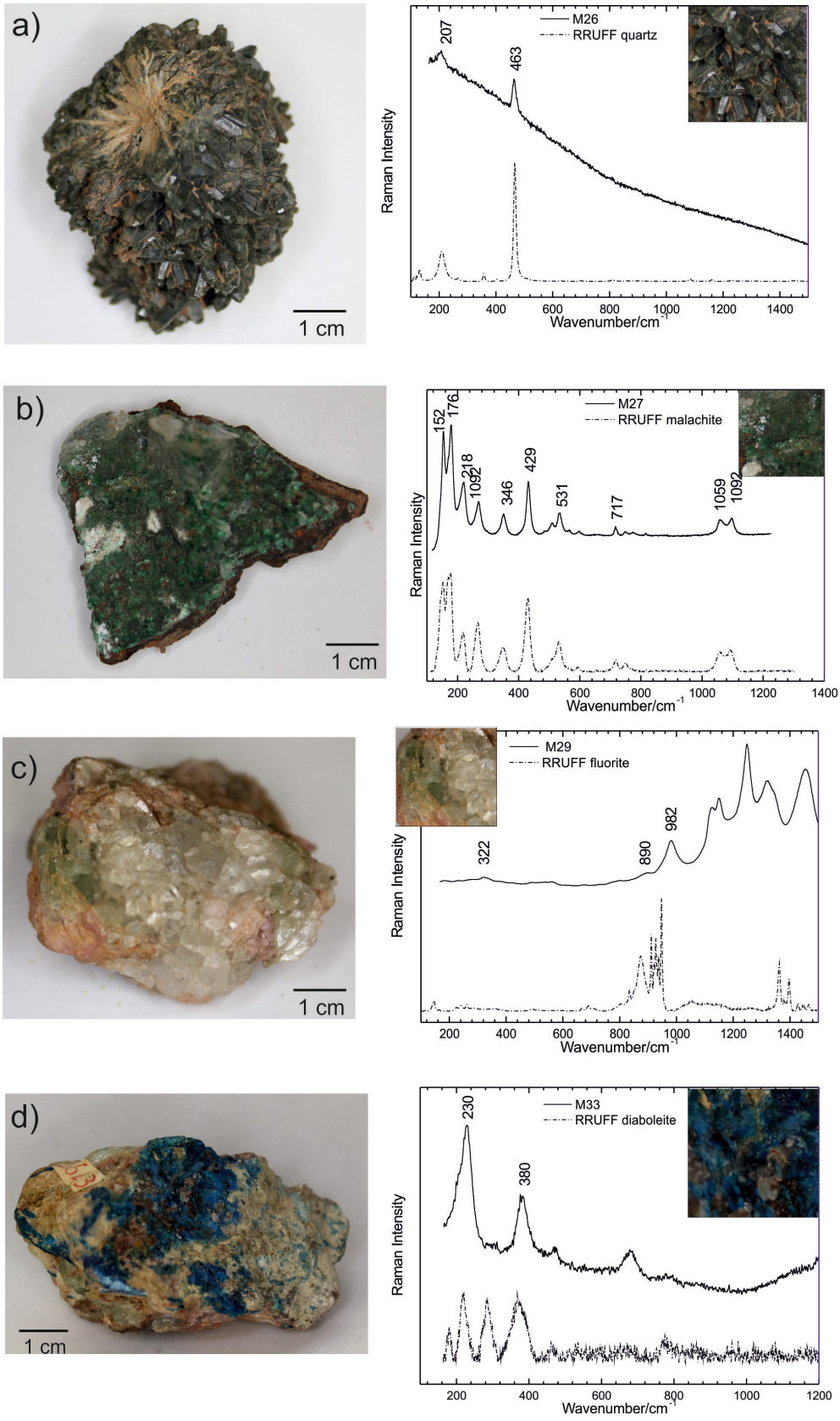

Fig. 2 - Picture and micro-Raman spectra acquired by using 785 nm excitation line on some misclassified materials, as examples. (a) sample M26: pyromorphite reclassified as black quartz; (b) sample M27: barthite reclassified as malachite; (c) sample M29: green garnet reclassified as fluorite; (d) sample M33: lazurite reclassified as diaboleite.

Misunderstanding related to macroscopic features can be hypothesised also for samples M25 (classified as albite with quartz), M29 (classified as garnet), M31 (classified as wolframite) and M33 (archive tag: lazurite) reclassified as calcite, fluorite (Fig. 2c), anatase and diaboleite (Fig. 2d), respectively, on the basis of their Raman features (see Annex 2).

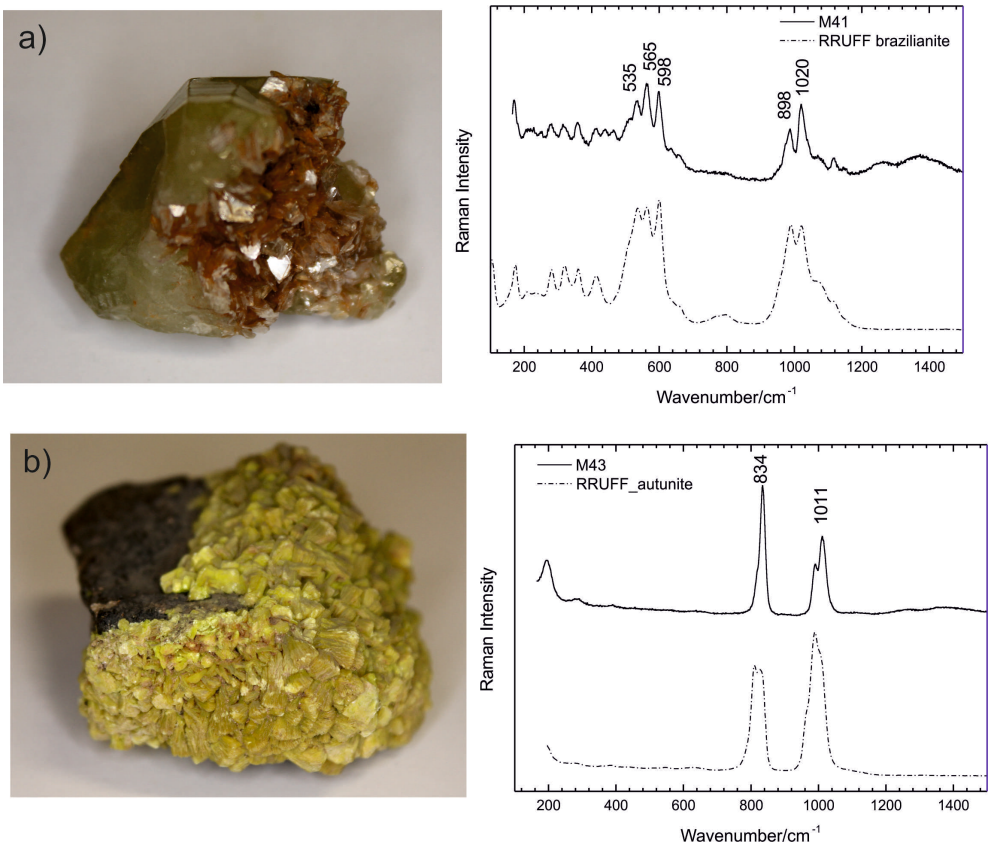

Fig. 3 - Picture and micro-Raman spectra (785 nm line) of (a) brazilianite and (b) autunite, as examples of correct classified mineralogical materials representative of phosphate mineral class.

Finally, a numerous and interesting set of phosphate and arsenate minerals (08; Nickel-Strunz Class), including minerals highly appreciated in gemological and collecting fields, has been identified. For almost of them, the comparison between the acquired Raman spectra and the reference ones available in the online databases has allowed to confirm the archive tags identification. As examples, quite nice brazilianite (M41) and amblygonite (M42) minerals, greatly used in gemology for their huge and luster features, and autunite (M43), a secondary mineral resulting from the oxidation of primary uranium minerals are shown in Fig. 3. Among phosphate minerals, noteworthy are samples labeled as M44 and M46, classified as purpurite and rashleighite-turquoise, respectively. For these minerals reference Raman spectra have not been recovered in the online databases and, therefore, the preliminary identification of the sample has been obtained on the basis of their X-ray diffraction pattern (Fig. 4).

Rashleighite-turquoise is a ferrian turquoise variety with formula $CuFe_6(PO_4)_4(OH)_8 \cdot 5H_2O$. Even if the turquoise group is widely studied in scientific literature, really poor data about crystal structure as well as Raman features of these minerals are provided (Frost *et al.*, 2006); moreover, no ferri-turquoise mineral reference spectra are available in the online databases. The Raman spectrum of rashleighite-turquoise acquired in the range 100-1800 cm^{-1} by using 785 nm line is shown in Fig. 4a. It is mainly characterized by phosphate modes (Frost &

Palmer, 2007); in detail, the ν_3 anti-symmetric stretching mode is due to two contributes centered at about 1017 and 1032 cm^{-1}, while the ν_4 mode is represented by a weak peak at 567 cm^{-1}.

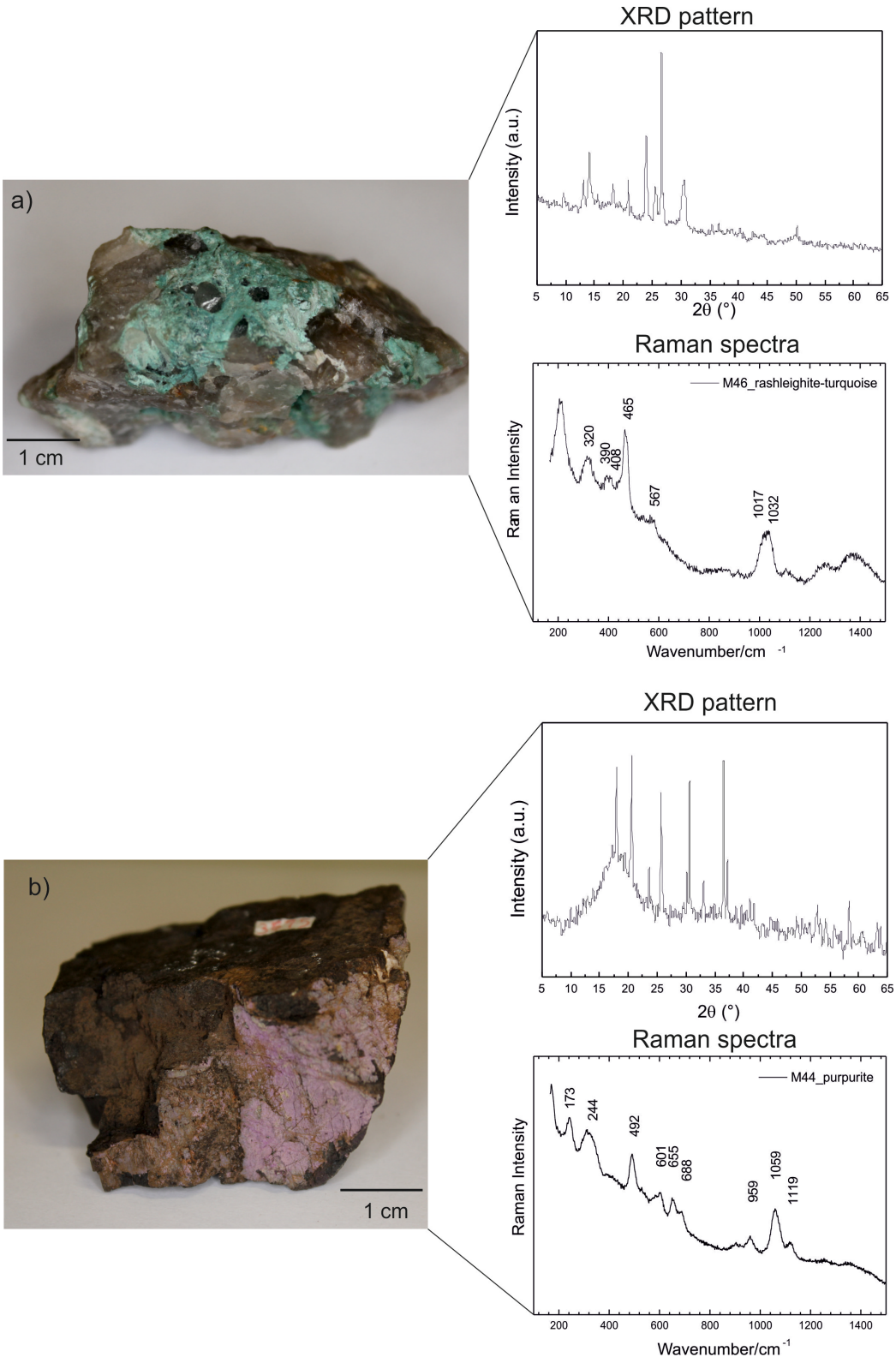

Fig. 4 - Picture, micro-Raman spectra (785 nm line) and XRD patterns of (a) rashleighite-turquoise and (b) purpurite samples.

In the region of the phosphate ν_2 anti. band. modes, three peaks at 390, 408 and 465 cm^{-1} can be identified; finally, a peak at about 320 cm^{-1} has been detected, related to CuO stretching vibrations (Annex 3).

Referring to purpurite, a Mn phosphate very popular as gemstone, actually it is mentioned in the list of samples needed for the improvement of the RRUFF database project (http://rruff.info/about/minerals_needed.php).

The acquired Raman spectrum of purpurite (see Fig. 4b and Annex 3) shows the typical modes of phosphate group. In detail, an intense band at 1059 cm^{-1}, attributed to the $(PO4)^{3-}$ ν_1 symmetric stretching mode can be observed; two bands are also visible at 959 and 1119 cm^{-1}, assigned to the $(PO_4)^{3-}$ ν_3 anti-symmetric stretching modes. In the 500-700 cm^{-1} region the spectrum of purpurite shows three bands at 601, 655 and 688 cm^{-1}, assigned to the ν_4 out of plane phosphate bending modes. Finally, in the 400-500 cm^{-1} range a band at 492 cm^{-1} and attributed to the $(PO_4)^{3-}$ ν_2 anti-symmetric bending mode can be identified, while between 300 and 100 cm^{-1} few bands related to lattice modes vibrations are detectable.

CONCLUSIONS

The overall spectroscopic data collected on unclassified and misclassified mineralogical samples discovered in the archives of the DBGES of Catania University allow to obtain all the basic information needed for the new cataloguing of the mineralogical collections.

Among them, the phosphate and arsenate class minerals represent a quite valuable and numerous set of materials, suitable for the staging of a new cabinet at the Mineralogical Museum in view of their relevance in gemology, collecting field, ore researches and economic applications as well as the beauty of the specimens. Finally, the presence of a rashleighite-turquoise and a purpurite samples has to be considered a quite valuable resource in the framework of the enlargement of Raman databases. In fact, the availability of their Raman spectra on online platforms can support the geological and mineralogical researches on phosphate minerals.

In conclusion, with this work we have demonstrated the potential of Raman spectroscopy in easy, fast, cheap, non-destructive and non-invasive identification of minerals in the framework of Natural Museum cataloguing, supplying also a quite valuable contribute to online RRUFF project.

REFERENCES

AA.VV. (2009): Regole italiane di catalogazione REICAT. Istituto centrale per il catalogo unico delle biblioteche italiane e per le informazioni bibliografiche, Roma, 632 p.

Adriaens, A. (2005): Non-destructive analysis and testing of museum objects: An overview of 5 years of research. *Spectrochim. Acta B*, **60**, 1503-1516.

Barone, G., Bersani, D., Crupi, V., Longo, F., Longobardo, U., Lottici, P.P, Aliatis, I., Majolino, D., Mazzoleni, P., Raneri, S., Venuti, V. (2014): A portable versus micro-Raman equipment comparison for gemmological purposes: the case of sapphires and their imitations. *J. Raman Spectrosc.,* **45**, 1309-1317.

Barone, G., Bersani, D., Jehlička, J., Lottici, P.P., Mazzoleni, P., Raneri, S., Vandenabeele, P., Di Giacomo, C., Larinà, G. (2015): Nondestructive investigation on the 17-18th centuries Sicilian jewelry collection at the Messina regional museum using mobile Raman equipment. *J. Raman Spectrosc.*, **46**, 989-995.

Bersani, D., Azzi, G., Lottici, P.P., Lambruschi, E., Barone, G., Mazzoleni, P., Raneri, S., Longobardo, U. (2014): Characterization of emeralds by micro-Raman spectroscopy. *J. Raman Spectrosc.*, **45**, 1293-1300.

Bouchard, M. & Smith, D.C. (2003): Catalogue of 45 reference Raman spectra of minerals concerning research in art history or archaeology, especially on corroded metals and coloured glass. *Spectrochim. Acta A*, **59**, 2247-2266.

Burgio, L. & Clark, R.J.H. (2001): Library of FT-Raman spectra of pigments, minerals, pigment media and varnishes, and supplement to existing library of Raman spectra of pigments with visible excitation. *Spectrochim. Acta A*, **57**, 1491-1521.

Frost, R.L. & Kloprogge, J.T. (2003): Raman spectroscopy of some complex arsenate minerals. Implications for soil remediation. *Spectrochim. Acta A*, **59**, 2797-2804.

Frost, R.L. & Palmer, S.J. (2007): A Raman spectroscopic study of the phosphate mineral pyromorphite $Pb_5(PO_4)_3Cl$. *Polyhedron*, **26**, 4533-4541.

Frost, R.L., Martens, W., Kloprogge, J.T., Ding, Z. (2003): Raman spectroscopy of selected lead minerals of environmental significance. *Spectrochim. Acta A*, **59**, 2705-2711.

Frost, R.L., Reddy, B.J., Martens, W., Weier, M. (2006): The molecular structure of the phosphate mineral turquoise - A Raman spectroscopic study. *J. Mol. Struct.*, **788**, 224-231.

Handbook of Minerals Raman spectra, Laboratoire de géologie de Lyon ENS, Lyon, France. http://ens-lyon.fr/LST/Raman [accessed 01 October 2016]

Hope, G.A., Woods, R., Munce, C.G. (2001): Raman microprobe mineral identification. *Min. Eng.*, **14**, 1565-1577.

Jehlička, J., Vítek, P., Edwards, H.G., Heagraves, M., Capoun, T. (2009): Application of portable Raman instruments for fast and non-destructive detection of minerals on outcrops. *Spectrochim. Acta A*, **73**, 410-419.

Kohlstedt, S.G. (1988): Curiosities and Cabinets: Natural History Museums and Education on the Antebellum Campus. *Isis*, **79/3**, 405-426.

Minerals Raman Database, Physics Department, University of Parma, Italy. http://www.fis.unipr.it/phevix/ramandb.php [accessed 01 October 2016].

Nasdala, L., Smith, D.C., Kaindl, R., Ziemann, M.A. (2004): Raman spectroscopy: Analytical perspectives in mineralogical research. *In*: "Spectroscopic methods in Mineralogy", A. Beran & E. Libowtzky, eds. *EMU Notes in Mineralogy*, **6**, 281-343.

Periasamy, A., Muruganand, S., Palaniswamy, M. (2009): Vibrational studies of Na_2SO_4, K_2SO_4, $NaHSO_4$ and $KHSO_4$ crystals. *Rasayan J. Chem.*, **2**, 981-989.

RRUFF Project, Department of Geosciences, University of Arizona, Tucson, USA. http://rruff.info/ [accessed 01 October 2016].

Smith, G.D. & Clark, R.J.H. (2004): Raman microscopy in archaeological science. *J. Archaeol. Sci.*, **31**, 1137-1160.

Vandenabeele, P. (2004): Raman spectroscopy in art and archaeology. *J. Raman Spectrosc.*, **35**, 607-609.

Vítek, P., Alib, E.M.A., Edwards, H.G.M., Jehlička, J., Cox, R., Page, K. (2012): Evaluation of portable Raman spectrometer with 1064 nm excitation for geological and forensic applications. *Spectrochim. Acta A*, **86**, 320-327.

ANNEX 1 - List of analysed minerals, with indication on archive tags and detailed description of some proprieties determined by preliminary macroscopic analysis as luster, color, diaphaneity and fracture.

Sample ID	*Archive tag (when present)*	*color*	*luster*	*diaphaneity*	*fracture*
M1	none	colorless	vitreous	transparent	sub-conchoidal
M2	none	reddish-orange	pearly	translucent	conchoidal
M3	none	white	vitreous	transparent	conchoidal
M4	none	light violet	vitreous	transparent	uneven
M5	none	deep red	vitreous	transparent	conchoidal
M6	none	deep red	metallic	opaque	uneven
M7	none	black	metallic	opaque	uneven
M8	none	white-gray	vitreous	transparent	conchoidal
M9	none	white	vitreous	transparent	conchoidal
M10	none	black	metallic	opaque	uneven
M11	none	light yellow	vitreous	transparent	conchoidal
M12	none	white	pearly	translucent	conchoidal
M13	none	black	metallic	opaque	uneven
M14	none	black	resinous	translucent	conchoidal
M15	none	reddish-brown	metallic	opaque	uneven
M16	none	reddish-brown	pearly	translucent	conchoidal
M17	none	green	vitreous	translucent	conchoidal
M18	none	deep green	vitreous	translucent	sub-conchoidal
M19	none	black	metallic	opaque	flaky
M20	none	red	vitreous	adamantine	uneven
M21	none	grayish	vitreous	tranlucent	splintery
M22	none	grayish	vitreous	tranlucent	uneven
M23	none	reddish brown	vitreous	tranlucent	conchoidal
M24	none	brown; yellow-brown	resinous	opaque	conchoidal
M25	quartz with albite	pink	vitreous	transparent	conchoidal
M26	none	black	vitreous	transparent	sub-conchoidal
M27	barthite	deep green	vitreous	tranlucent	sub-conchoidal
M28	fluorite	from white to pink	pearly	translucent	conchoidal
M29	garnet	light green	vitreous	transparent	conchoidal
M30	red quartz	reddish-brown	metallic	opaque	sub-conchoidal
M31	wolframite	reddish-brown	vitreous	translucent	conchoidal
M32	fluorite with quartz	black	metallic	opaque	sub-conchoidal
M33	lazurite	blue	vitreous	subtranslucent to opaque	uneven
M34	anglesite	black	vitreous	translucent	conchoidal
M35	wavellite	light green	pearly	translucent	uneven
M36	pyromorphite	light green	resinous	translucent	sub-conchoidal
M37	limonite -pirite	reddish-brown	metallic	opaque	uneven
M38	hambergite	white	vitreous	translucent	conchoidal
M39	cuproadamite	green	vitreous	translucent	uneven
M40	roselite	from dark rose to pink	vitreous	transparent	conchoidal
M41	brazilianite	light yellow	vitreous	transparent	conchoidal
M42	amblygonite	grayish	vitreous	tranlucent	uneven
M43	autunite	greenish yellow	vitreous	transparent	uneven
M44	purpurite	violet	earthy	subtranslucent	uneven
M45	xenotime	yellow-brown	vitreous	opaque	splintery
M46	rashleighite	blue-green	waxy	subtranslucent	conchoidal

ANNEX 2 - Raman analysis results and compositional attribution of studied samples. The new cataloguing information obtained thanks to the identification of the studied mineralogical samples are also reported (Cont'd).

		Raman analysis results		New cataloguing information			
Sample ID	***Previous classification***	***Raman features (cm^{-1})***	***Attribution***	***Category***	***Formula***	***Crystal symmetry***	***Strunz classification***
M1	Unclassified	710, 1084	aragonite	Carbonate mineral	$CaCO_3$	Trigonal	05.AB.15
M2	Unclassified	280, 710, 1087	calcite	Carbonate mineral	$CaCO_3$	Trigonal	05.AB.05
M3	Unclassified	210, 463	quartz	Oxide mineral	SiO_2	Trigonal	04.DA.05
M4	Unclassified	711	lepidolite	Silicate mineral	$K(Li,Al)_3(Si,Al)_4O_{10}(F,OH)_2$	Monoclinic	09.EC.20
M5	Unclassified	196, 306, 731, 1089	sphaerocobaltite	Carbonate mineral	$CoCO_3$	Trigonal	05.AB.05
M6	Unclassified	226, 292, 409, 494, 610	hematite	Oxide mineral	Fe_2O_3	Trigonal	04.CB.05
M7	Unclassified	292, 410	hematite	Oxide mineral	Fe_2O_3	Trigonal	04.CB.05
M8	Unclassified	153, 281, 712, 1086	calcite	Carbonate mineral	$CaCO_3$	Trigonal	05.AB.05
M9	Unclassified	206, 464	quartz	Oxide mineral	SiO_2	Trigonal	04.DA.05
M10	Unclassified	231, 297, 414, 616, 666	hematite	Oxide mineral	Fe_2O_3	Trigonal	04.CB.05
M11	Unclassified	156, 282, 714, 1088	calcite	Carbonate mineral	$CaCO_3$	Trigonal	05.AB.05
M12	Unclassified	453, 624, 1000	celestine	Sulfate mineral	$SrSO_4$	Ortho-rhombic	07.AD.35
M13	Unclassified	295, 408, 552, 614	hematite; goethite	Oxide mineral	Fe_2O_3; $FeO(OH)$	Trigonal; orthorombic	04.CB.05
M14	Unclassified	446, 607	chloroapatite	Phosphate mineral	$Ca_5(PO_4)_3Cl$	Hexagonal	08.BN.05
M15	Unclassified	225, 297, 405	hematite	Oxide mineral	Fe_2O_3	Trigonal	04.CB.05
M16	Unclassified	291, 1090	siderite	Carbonate mineral	$FeCO_3$	Trigonal	05.AB.05
M17	Unclassified	389, 483	analcime	Silicate mineral	$NaAlSi_2O_6 \cdot H_2O$	Cubic	09.GB.05
M18	Unclassified	323	fluorite	Halide mineral	CaF_2	Isometric	03.AB.25
M19	Unclassified	1330, 1586	graphite	Native element mineral	C	Hexagonal	
M20	Unclassified	260, 351	cinnabar	Sulfide mineral	HgS	Trigonal	02.CD.15
M21	Unclassified	231, 297, 414, 501, 613, 963, 1005, 1070	wagnerite	Phosphate mineral	$(Mg,Fe)_2(PO_4)F$	Monoclinic	08.BB.15
M22	Unclassified	815, 1032, 1050	mimetite	Phosphate mineral	$Pb_5(AsO_4)_3Cl$	Hexagonal	08.BN.10
M23	Unclassified	211, 260, 350, 380, 464, 497, 547, 740, 810, 850	carminite	Arsenate mineral	$PbFe^{3+}_2(AsO_4)_2(OH)_2$	Orthorhombic	08.BH.30
M24	Unclassified	1149, 1269, 1475, 1602, 1730	monazite	Phosphate mineral	$(Ce,La,Y,Th)PO_4$	Monocline	08.AD.50
M25	quartz with albite	153, 280, 710, 1084	calcite	Carbonate mineral	$CaCO_3$	Trigonal	05.AB.05
M26	pyromorphite Assau	207, 463	black quarz	Oxide mineral	SiO_2	Trigonal	04.DA.05
M27	barthite	152, 176, 218, 266, 346, 429, 531, 717, 1059, 1092	malachite	Carbonate mineral	$Cu_2CO_3(OH)_2$	Monoclinic	05.BA.10
M28	fluorite	169, 292, 724, 1095	dolomite	Carbonate mineral	$CaMg(CO_3)_2$	Trigonal	05.AB.10
M29	garnet	322, 890, 982	fluorite	Halide	CaF_2	Isometric	03.AB.25
M30	red quartz	225, 295, 411, 613	hematite	Oxide mineral	Fe_2O_3	Trigonal	04.CB.05

ANNEX 2 - (Continued)

		Raman analysis results		New cataloguing information			
Sample ID	***Previous classification***	***Raman features (cm^{-1})***	***Attribution***	***Category***	***Formula***	***Crystal symmetry***	***Strunz classification***
M31	wolframite	145	anatase	Oxide mineral	TiO_2	Tetragonal	04.DD.05
M32	fluorite with quartz	227, 294, 414, 499, 615	hematite	Oxide mineral	Fe_2O_3	Trigonal	04.CB.05
M33	lazulite	230, 380	diaboleite	Halide mineral	$Pb_2CuCl_2(OH)_4$	Tetragonal	03.DB.05
M34	anglesite	437, 604, 640, 977, 1058, 1158	anglesite	Sulphate mineral	$PbSO_4$	Orthorhombic	07.AD.35
M35	wavellite	280, 315, 413, 1022	wavellite	Phosphate mineral	$Al_3(PO_4)_2(OH,F)_3 \cdot 5H_2O$	Orthorhombic	08.DC.50
M36	pyromorphite	393, 417, 918, 942	pyromorphite	Phosphate mineral	$Pb_5(PO_4)_3Cl$	Hexagonal	08.BN.05
M37	limonite -pirite	302, 402, 551	limonite	Amorphous, mineraloid	$FeO(OH) \cdot nH_2O$	-	Unclassified
M38	hambergite	156, 285, 396, 987	hambergite	Borate mineral	Be_2BO_3OH	Orthorhombic	06.AB.05
M39	cuproadamite	300, 403, 807	cuproadamite	Arsenate mineral	Zn_2AsO_4OH	Orthorhombic	08.BB.30
M40	roselite	215, 390, 450, 798, 854	roselite	Arsenate mineral	$Ca_2(Co,Mg)(AsO_4)_2 \cdot 2(H_2O)$	Monoclinic	08.CG.10
M41	brazilianite	535, 565, 598, 989, 1020	brazilianite	Phosphate mineral	$NaAl_3(PO_4)_2(OH)_4$	monoclinic	08.BK.05
M42	amblygonite	288, 477, 505, 642, 815, 1031	amblygonite	Phosphate mineral	$(Li,Na)AlPO_4(F,OH)$	Triclinic	08.BB.05
M43	autunite	834, 1011	autunite	Phosphate mineral	$Ca(UO_2)_2(PO_4)_2 \cdot 10\text{-}12H_2O$	Orthorhombic	08.EB.05
M44	purpurite	173, 244, 308, 366, 492, 601, 655, 688, 959, 1059, 1119	purpurite	Phosphate mineral	$MnPO_4$	Orthorhombic	08.AB.10
M45	xenotime	259, 307, 579, 1345, 1407, 1517	xenotime	Phosphate mineral	$Y(PO_4)$	Tetragonal	08.AD.35
M46	rashleighite	320, 390, 408, 465, 567, 1017, 1032	rashleighite	Phosphate mineral	$CuFe_6(PO_4)_4(OH)_8 \cdot 5H_2O$	Triclinic	08.DD.15

ANNEX 3 - Raman Vibrational Raman frequencies of rashleighite-turquoise and purpurite samples.

Rashleighite-turquoise, ferrian turquoise: $CuFe_6(PO_4)_4(OH)_8 \cdot 5H_2O$		
Symmetry class	**Type of mode**	**Raman frequency (cm^{-1})**
CuO	stretching	320 (m)
$\nu_2 (PO_4)^{3-}$	anti. bend.	390 (m)
$\nu_2 (PO_4)^{3-}$	anti. bend.	408 (m)
$\nu_2 (PO_4)^{3-}$	anti. bend.	465 (s)
$\nu_4 (PO_4)^{3-}$	sym. bend.	567 (w)
$\nu_3 (PO_4)^{3-}$	anti. stretch.	1017 (**vs**)
$\nu_3 (PO_4)^{3-}$	anti. stretch.	1032 (s)
Purpurite: $MnPO_4$		
Symmetry class	**Type of mode**	**Raman frequency (cm^{-1})**
\	lattice mode	244 (m)
\	lattice mode	308 (m)
\	lattice mode	366 (m)
$\nu_2 (PO_4)^{3-}$	anti. bend.	492 (s)
$\nu_4 (PO_4)^{3-}$	sym. bend.	601 (m)
$\nu_4 (PO_4)^{3-}$	sym. bend.	655 (s)
$\nu_4 (PO_4)^{3-}$	sym. bend.	688 (sh)
$\nu_3 (PO_4)^{3-}$	anti. stretch.	959 (m)
$\nu_1 (PO_4)^{3-}$	sym. stretch.	1059 (**vs**)
$\nu_3 (PO_4)^{3-}$	anti. stretch.	1119 (m)